[논 문] 한국재료학회지
Korean Journal of Materials Research
Vol. 8, No. 4 (1998)

Contact Fracture behavior of Silicon Nitride Bilayer

Kee Sung Lee, Seung Kun Lee* and Do Kyung Kim

Dept. of Materials Science and Engineering, KAIST, Taejon, 305-701
**Materials Science and Engineering Laboratory,*
National Institute of Standards and Technology, Gaithersburg, MD20899, USA

질화규소 이층 층상재료의 접촉파괴거동

이기성 · 이승건* · 김도경
한국과학기술원 재료공학과
*미국 표준과학연구소

(1997년 11월 14일 받음, 1997년 12월 22일 최종수정본 받음.)

Abstract The fracture behavior of Si_3N_4 coated Si_3N_4-BN composite was studied by the Hertzian indentation technique. New types of contact-induced cracks were found, and it was confirmed that these cracks have cone crack geometry. Contact damage was distributed in the substrate layer, which can absorb energy, as well as in the coating layer, so the propagation of initiated cracks in the coating layer were suppressed.

초 록 질화규소로 코팅된 질화규소-질화붕소 이층 층상복합재료의 접촉하중에 의한 파괴거동을 고찰하였다. 그 결과 코팅층 내에서 새로운 종류의 균열들이 발견되었고, 이러한 균열들은 기하학적으로 원추 모양을 가짐을 확인하였다. 외부에서 가한 하중의 에너지는 코팅층 뿐 아니라 damage를 흡수할 수 있는 기판층 내로 분산되어 코팅층에서 시작된 균열들의 전파가 억제되었다.

1. Introduction

Si_3N_4-BN composite is increasingly being used for thermal barrier and thermal shock resistant material because of its excellent thermal resistance.[1] In addition, the weak interface provides crack deflection and bridging, so leads to improvement in fracture toughness and damage tolerance.[2] However, the strength and hardness of Si_3N_4-BN composite are lower than those of monolithic Si_3N_4 material. Weak interface in Si_3N_4-BN composite may enhance the material removal on a micro-scale, reduce the strength, and deteriorate the wear resistance. Therefore this material requires a hard coating.[3]

When the hard layer is coated on the soft layer, contact-induced fracture becomes important. Recently, extensive researches have focused on hard ceramic layer coating on a soft metal layer. However, most of the research has concentrated mostly on fracture during fabrication or fracture directly after fabrication. For example, failure behaviors by residual stress in a system with weak interface are of interest in practical coating systems.[4~6] Our interest in the bilayer, hard coating on soft substrate layer, is to demonstrate the fracture driven by contact when the bilayer is situated under the compressive stress. Such concentrated stresses are especially pertinent to ceramic engine components, cutting tools, and bearing applications.

There has been no systematic study of contact-induced fracture on a hard coating/soft substrate layer system.

Consequently, in this research, Si_3N_4/Si_3N_4-20wt% BN bilayer with strong interface was fabricated by hot pressing to exclude the effect of delamination of the interface. We specially used the Hertzian indentation technique to induce the contact fracture in the coating layer.[7,8] The behavior of the contact fracture was evaluated by increasing the applied load using spherical indenter. Although brittle ceramic produces only cone crack from the surface,[7,8] three contact-induced cracks were identified in this study ; the transverse crack from the interface between the coating and the substrate layer, the crack with an S shape from the middle of the coating layer, and finally the classical cone crack from the surface. Attention focused on crack propagation rather than crack initiation. We will propose that all contact-induced cracks can be considered as a cone-geometry.

The effect of a damage-absorbent substrate layer on fracture behavior and damage distribution was also

studied. The coating thickness was varied 250 and 400 μm to study the effect of the substrate layer.

2. Experimental Procedure

2.1. Sample preparation and characterization

Si_3N_4 coated Si_3N_4-20wt%BN bilayer was fabricated by powder preparation, stacking and hot pressing. In order to prepare the powder for the substrate layer, BN powder (Aldrich Chemical, Milwaukee, WI, U.S.A.) was mixed with a Si_3N_4 powder mixture during powder preparation. The Si_3N_4 starting powder mixture was Si_3N_4 (UBE-SN-E10, Ube Industries, Japan) with sintering additives of 2wt% Al_2O_3(AKP50, Sumitomo Chemical Co. Ltd., Tokyo, Japan), 5wt% Y_2O_3(H.C.Starck GmbH, Goslar, Germany) and 1wt% MgO (High Purity, Baikowski Co., NC, U.S.A.). For the coating layer, a Si_3N_4 powder mixture including the same type and amount of sintering additives was used. Each powder batch was ball milled using alumina balls in isopropanol for 24 hr and then dried in the oven and sieved.

Each powder mixture was stacked in the graphite mold and hot pressed to fabricate the bilayer of coating thickness of 1~2mm and substrate thickness of 3mm with a strongly bonded interface at 1730℃ under 30MPa for 1 hr. Each specimen was ground and the surface was polished to 1μm to control the coating thickness. Coating thickness was controlled up to 250 and 400μm, respectively.

Plasma etching was performed to reveal the microstructure, and microstructural examination was carried out by scanning electron microscopy (SEM). Archemedes principle confirmed the sintered density. Basic material characterization was performed by Vickers indentation. Hardness and toughness were measured for individual layer materials.

2.2. Hertzian indentation

A simple Hertzian indentation was made on polished surfaces to evaluate properties and induce the cone crack from the surface. Elastic modulus and yield stress of individual layer materials were measured from indentation stress-strain curves.[9] Test surfaces were gold coated before indentation to facilitate measurement of contact radius a at the given load P using an indenter with a radius of indenter, r. Indentation stress ($p_0 = P/\pi a^2$) and indentation strain (a/r) were calculated after measuring contact radius a, at the given load P, and then the indentation stress-strain curve was plotted. The elastic modulus could be determined from the initial slope in the elastic region of indentation stress-strain curves. Indentations were also made on each composite to determine critical loads P_Y by first residual impressions, and then yield stress Y, from $p_Y = P_Y/\pi a^2 = 1.1Y$

The side surface was polished to 1μm diamond paste finish, to confirm the strong interface. WC ball with radius of 1.98mm was indented across the interface at P = 1000N and 1500N.

Each specimen was cut in 3mm×4mm×25mm, polished and bonded together to make the bonded-specimen for characterizing of contact damage beneath the surface. Hertzian indentations were made on the center of the interface in the bonded-specimen using a WC ball with a radius of 1.98mm at an increasing load from P=1500~4000N. After that, the bond was dissolved in acetone and the subsurface was examined by Nomarski illumination using an optical microscope. The cone crack length and depth at each load condition were measured with an optical microscope. Continuous polishing was conducted from the top surface to determine the crack geometry.

3. Results and Discussion

3.1. Material characterization

Figure 1 shows the microstructure of a Si_3N_4 coated Si_3N_4-20wt%BN bilayer. The top layer corresponds to the coating layer, and the bottom layer, including the plate-like voids, is the substrate layer. The voids correspond to BN sites because BN evaporates during plasma etching process. Throughout the specimen, BN platelets with 1.5~10μm diameter and 0.2~0.6μm thickness are well distributed and aligned in a parallel direction to the interface. The alignment of the platelets is

Fig. 1. SEM micrograph of Si_3N_4 coated Si_3N_4-20wt%BN bilayer composite : top layer is coating layer, and bottom layer including BN phase(dark phase) is substrate layer.

Table 1. Characteristics of Si_3N_4 and SiN-20wt%BN composites.

Material	Si_3N_4	Si_2N_3-20wt%BN
Relative density	>99%	>99%
Hardness, H(GPa)	14.6±0.5	7.4±0.4
Toughness* T_o(MPam$^{1/2}$)	5.3±0.6	7.6±0.6
Elastic modulus, E(GPa)	320±64	160±32
Yield stress, Y(GPa)	8.4±0.15	2.8±0.35

*for parallel radial crack to hot press direction

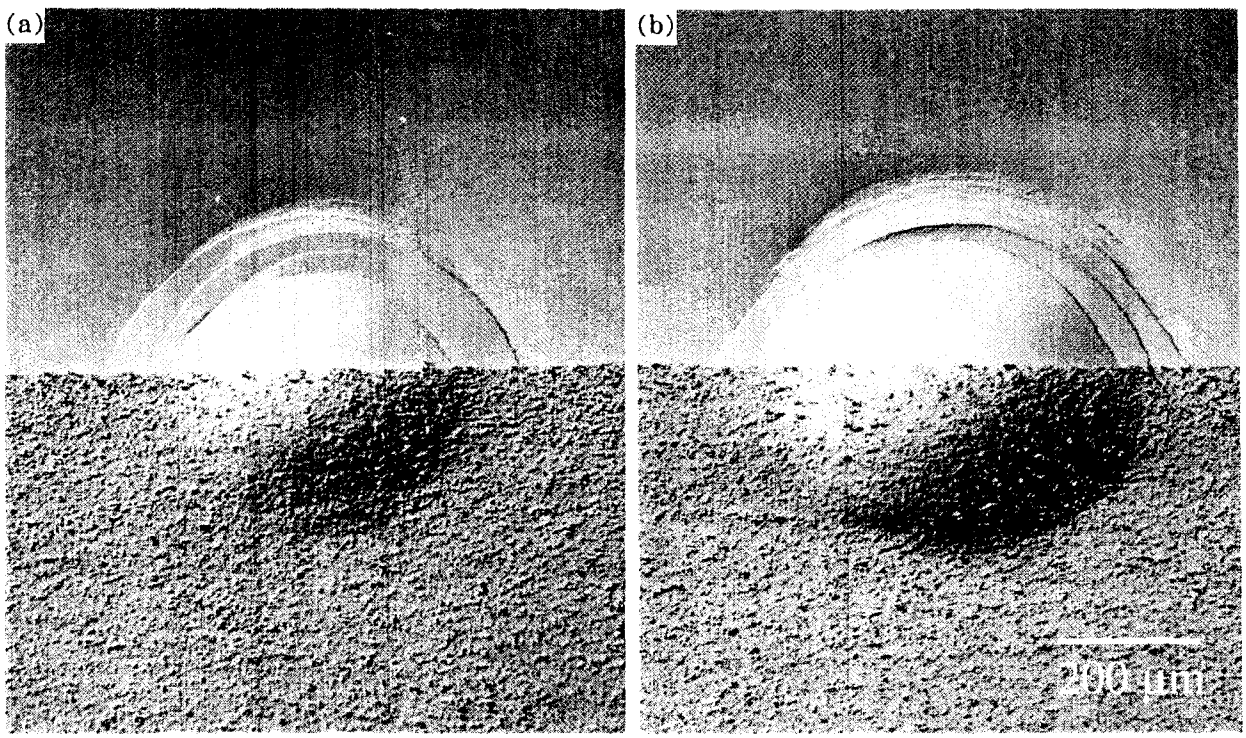

Fig. 2. Hertzian indentations on side surface of bilayer, made symmetrically across the interface, with WC sphere r=1.98mm at (a) P=1000N, and (b) P=1500N.

believed to be due to the movement of the platelets during hot pressing.

The characteristics of individual layer material are shown in Table 1. Hardness of substrate material (Si_3N_4-20wt%BN composite) is lower but toughness for a direction parallel to hot press is higher than coating material (Si_3N_4). This indicates Si_3N_4 is a good material for hard coating, and Si_3N_4-BN is an appropriate substrate material due to its relatively high toughness. Note that the elastic modulus and yield stress of Si_3N_4-BN material are lower than those of Si_3N_4 coating material.

Optical micrographs after P=1000N and P=1500N indentations are shown in Fig. 2. The fact that the interface delamination was not examined at the given loads, indicates that this bilayer has strong interface. Note the surface impression on the substrate side without ring cracking. Although the ring crack is produced in the hard but brittle layer, the crack is suppressed in soft and tough layer. This fact foreshadows the possibility of crack suppression by energy absorption in the substrate.

3.2. Fracture pattern analysis

Figure 3 shows side views of contact damage for Si_3N_4 coated Si_3N_4-20wt%BN bilayer. The variable is an indentation load, P=1500, 2000, 3000 and 4000N at constant coating thickness of 400μm. Completely different types of cracks compared to classical cone cracks were observed in the coating layer. First, a transverse crack (v) is examined from the interface between coating/substrate layer (P=1500N). The propagation direction is upward after the crack initiates from the interface. A second new type is an S-shaped crack (s) in the middle of the coating layer (P=2000N). As the region beneath the surface is compressed, the S-shape crack is initiated in the middle, and extends downward and upward at the same time. Finally, at higher load (P=3000N), a

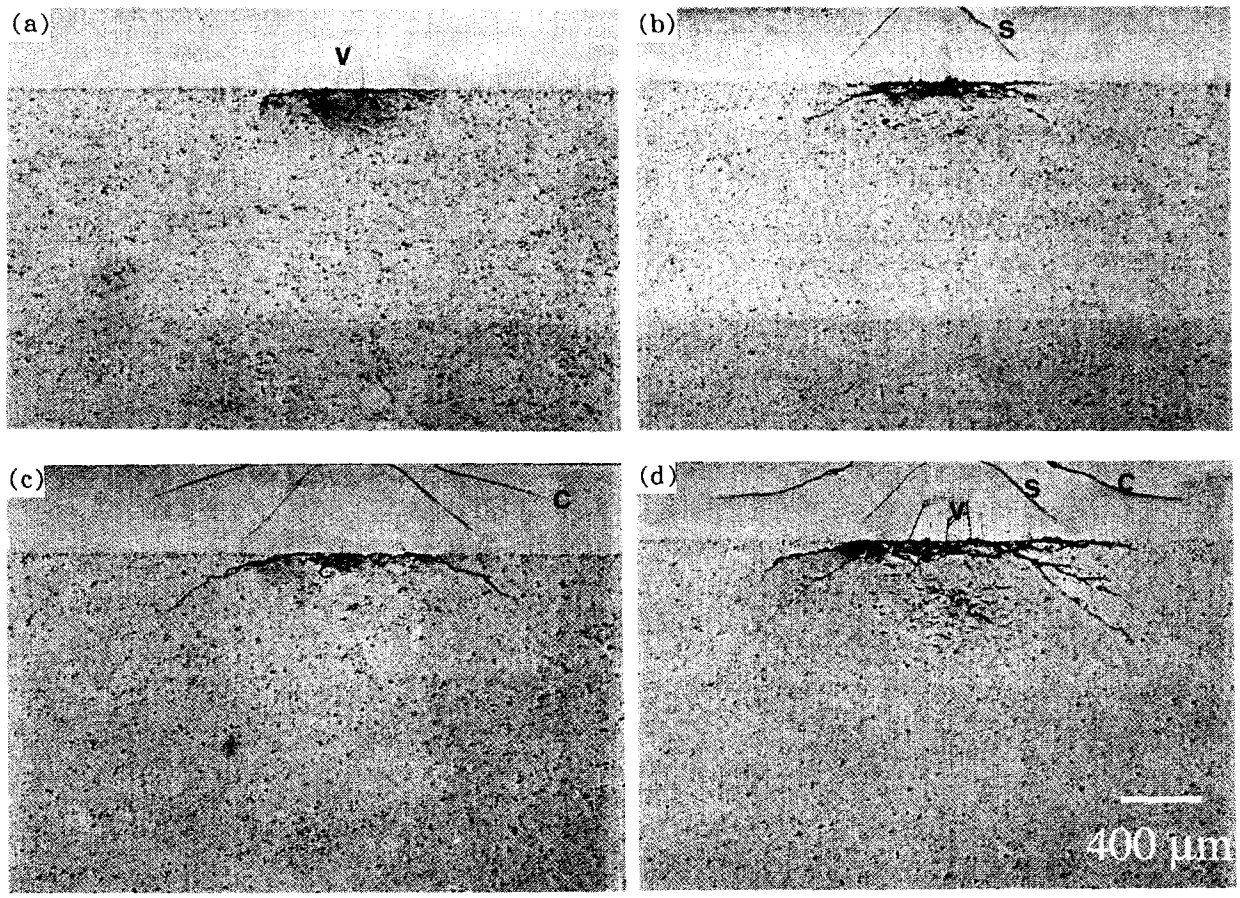

Fig. 3. Contact fracture of 400㎛ Si_3N_4 coated Si_3N_4-20wt%BN bilayer composites, using WC sphere r=1.98mm, showing effect of indentation applied load : (a) P=1500N, (b) P=2000N, (c) P=3000N, (d) P=4000N.

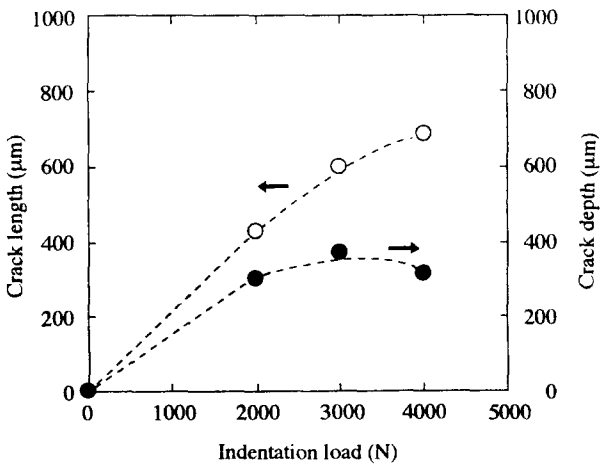

Fig. 4. Plot of cone crack length and depth as a function of indentation load for 400㎛ Si_3N_4 coated Si_3N_4-20wt%BN bilayer, using WC sphere with r=1.98mm.

classical cone crack(c) is observed from the surface. However, most of cracks are stable, so the cracks do not easily penetrate the interface. Other cracks from the interface into the substrate are found at higher loads instead of crack penetration. Even at the highest load(P=4000N), the bilayer does not fracture catastrophically. The cracks in the coating layer propagate along the direction parallel to interface. This result is quantified in Fig. 4. The longest crack length and the deepest crack depth in the coating layer were plotted as a function of indentation load. Whereas the crack length increases as increasing the applied load, the crack depth is almost constant with the increasing indentation load. This indicates that cracks do not propagate into the substrate and are arrested in the coating layer.

Figure 5 shows the cone crack geometry for these cracks. Top and side views after (a) 200㎛ grinding, and (b) 300㎛ grinding are shown in figure. These results confirm that all new crack types are cone crack geometry.

Figure 6 shows an enlarged micrograph of the damage zone in the coating layer. The damage zone in the coating layer is mostly formed at the central region of the S-shape crack. It is well known that the damage zone is driven by shear stress.[10] The S-shape crack is initiated in the middle of the coating layer, where the

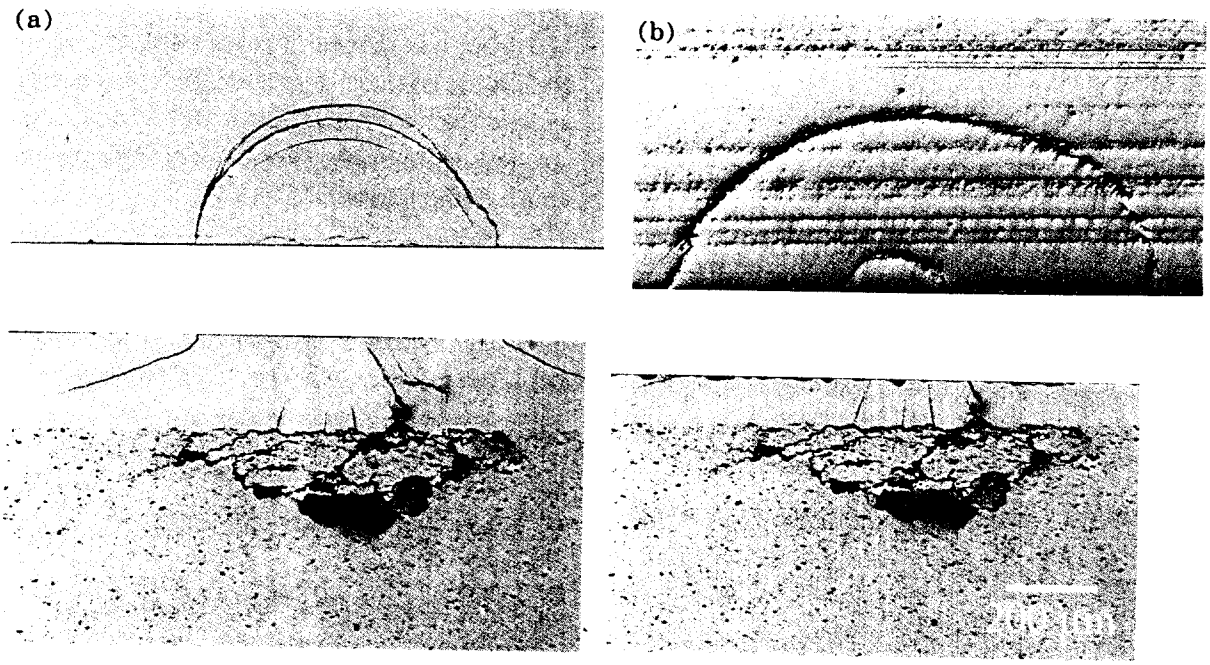

Fig. 5. Micrographs showing cone crack geometry after thickness grinding : (a) top and side view(bottom) after 200㎛ grinding, (b) top and side view(bottom) after 300㎛ grinding in 400㎛ Si_3N_4 coated Si_3N_4-20wt%BN composites.

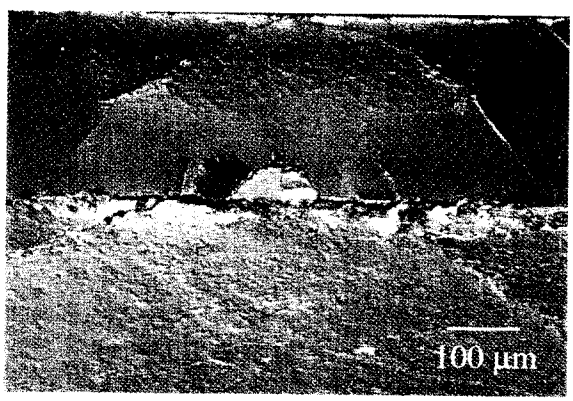

Fig. 6. Distributed damage zone in coating layer of 250㎛ Si_3N_4 coated Si_3N_4-20wt%BN composites.

shear stress is maximum. And then the cracks extend upward and downward at the same time. Substantial damage also occurs in the subsurface of the bilayer. Note that the damage zone is extended as the indentation load increases (Fig. 3). Prior research showed that the extensive damage zone can be formed in the material showing "quasi-plasticity".[11] This damage absorption contributes to cone crack suppression and/or arrest.

In a thinner coated bilayer with coating thickness d =250㎛, the flexural bending phenomena was observed in Fig. 7. Figure 7(a) shows the subsurface damage view after indentation was applied at P=2000N. As the indentation load increases up to 3000N, the coating layer begins to bend over (Fig. 7(b)), and this flexural phenomena is more severe when the load is higher, P= 4000N (Fig. 7(c)). Arrows indicate the flexural bending of coating layer due to the relative softness of substrate layer. In comparison with Fig. 3, the transverse crack densities increased in the coating layer because flexural bending brings larger tensile stress in the region of interface, that is, bottom region of coating material. However, the cracks are still arrested by compressive stresses and extensive damage absorptions in the substrate layer. Consequently, the transverse cracks are produced by this flexural bending but all cracks in the coating layer are suppressed by the substrate layer. The flexural bending is a major cause of crack initiation in the coating layer and extensive damage zone of the substrate layer contributes to the suppression of crack propagation.

4. Conclusion

The Hertzian contact damage in Si_3N_4/Si_3N_4-BN bilayer was investigated by spherical indenter. No interface delamination under contact pressure indicates strong interface between the two layers.

A new crack systems were found ; a transverse crack from the interface, an S-shaped crack from the middle of the coating layer, and a classical cone crack from the surface. The formation of these cracks is attributed to flexural bending stress caused by elastic-plastic mismatch between the two layers. These new crack types also have a three-dimensional cone crack

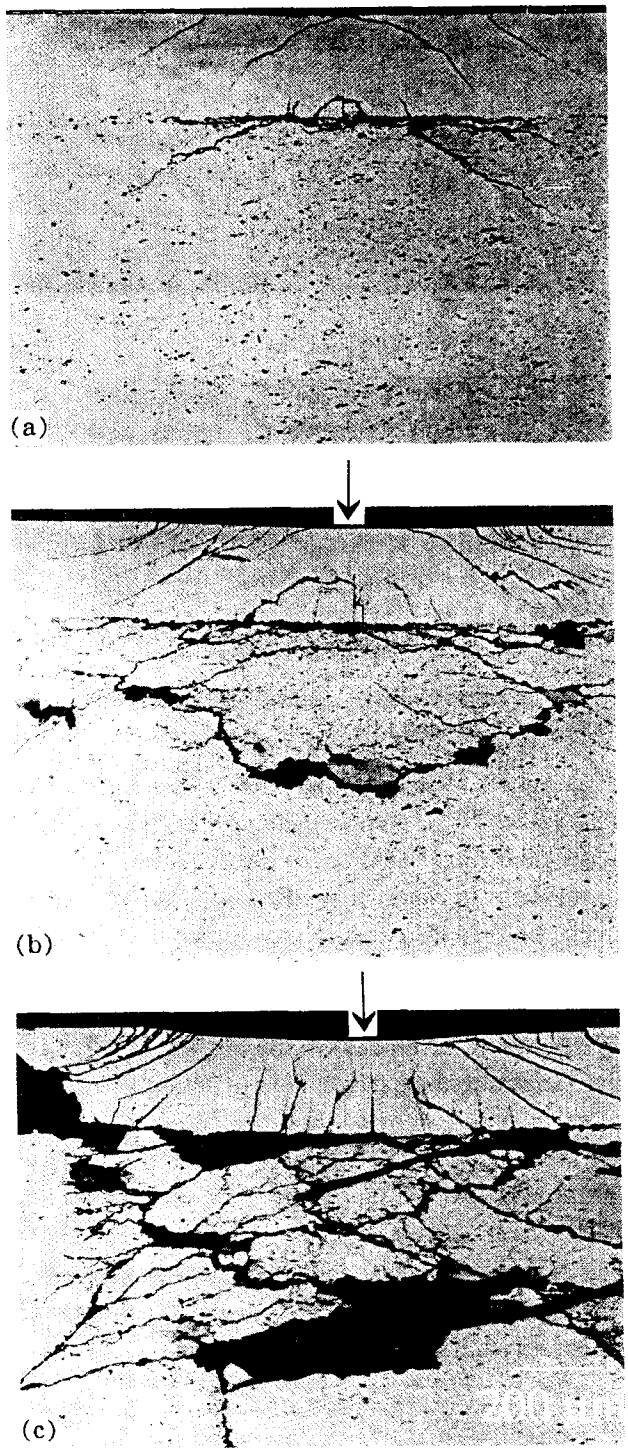

Fig. 7. Contact fracture of 250㎛ Si_3N_4 coated Si_3N_4-20wt%BN bilayer composites, using WC sphere r=1.98mm : (a) P=2000N, (b) P=3000N, (c) P=4000N.

shape.

Damage was distributed in the subsurface as well as the coating layer, so cone crack depth was nearly constant as the contact load increased. The stable cracks in coating and substrates foreshadow contact damage tolerance of this bilayer.

Acknowledgements

We acknowledge B. R. Lawn in NIST for his support, and thanks to Shi-Woo Lee and Jae-Hun Kim for helpness with the plasma etching and SEM analysis.

References

1. E. H. Lutz and M. V. Swain, J. Am. Ceram. Soc., **75** (1) 67 (1992)
2. S. Baskaran, S. D. Nunn, D. Popovic, and J. W. Halloran, J. Am. Ceram. Soc., **76** (9) 2209 (1993)
3. N. P. Padture and B. R. Lawn, Acta metall. mater., **43** (4) 1609 (1995)
4. A. K. Shinha, H. J. Levinstein, and T. E. Smith, J. Appl. Phys., **49** (4) 2423 (1978)
5. P. Scardi, M. Leoni, L. Bertamini, Thin Solid Films, **278** 96 (1996)
6. A. G. Evans and J. W. Hutchinson, Int. J. Solids Structures, **20** (5) 455 (1984)
7. A. Pajares, L. Wei, B. R. Lawn, N. P. Padture, and C. C. Berndt, Materi. Sci. Eng., **A208** (2) 158 (1996)
8. A. Pajares, L. Wei, B. R. Lawn, and C. C. Berdnt, J. Am. Ceram. Soc., **79** (7) 1907 (1996)
9. F. Guiberteau, N. P. Padture, H. Cai and B. R. Lawn, Phil. Mag. A, **68** (5) 1003 (1993)
10. Z. C. Xia and J. W. Hutchinson, Int. J. Solids. Structures **31** (8) 1133 (1994)
11. K. S. Lee S. K. Lee and D. K. Kim, "Quasi-Plasticity of Si_3N_4-BN Composites", Korean Journal of Materials Research, Vol. NO. pp (1997).